Mathematical modeling of preadipocyte fate determination

Huseyin Coskun[a,*], Taryn L.S. Summerfield[b], Douglas A. Kniss[c,b], Avner Friedman[d,a]

[a] *Mathematical Bioscience Institute, Ohio State University, Columbus, OH*
[b] *Obstetrics and Gynecology, (Laboratory of Perinatal Research), Ohio State University, Columbus, OH*
[c] *Departments of Biomedical Engineering, Ohio State University, Columbus, OH*
[d] *Department of Mathematics, Ohio State University, Columbus, OH*

Abstract

White adipose tissue is the major energy storage depot for neutral lipids and is also a key endocrine regulator of a host of homeostatic activities, including metabolism, feeding behaviors, cardiovascular functions and reproduction. Abnormal fat accretion in the setting of obesity can lead to insulin resistance and type 2 diabetes, and has been linked to some cancers and arteriosclerosis. Thus, a thorough appreciation of the intricate signaling events that must take place as quiescent adipocyte precursors are recruited into the proliferating cell population that then must 'decide' to differentiate into fully functional fat cells is critical to our understanding of diseases related to excess adipogenesis. We are beginning to gain insights into the molecular regulators of adipocyte differentiation. A significant advance would be to construct mathematical modeling tools that would assist cell biologists in predicting how environmental and/or intrinsic inputs could influence preadipocyte fate decision making. We have developed a model of how preadipocytes may use the dynamic interplay of two transcription factors, nuclear factor-κB (NF-κB) and peroxisome proliferator-activated receptor-γ (PPAR-γ) in early proliferation and differentiation events in vitro. Critical to the model is the feedback signaling between NF-κB and its inhibitor, IκB. The model is based

*To whom correspondence should be addressed

Email addresses: hcoskun@mbi.ohio-state.edu (Huseyin Coskun), summerfield.7@osu.edu (Taryn L.S. Summerfield), kniss.1@osu.edu (Douglas A. Kniss), afriedman@math.ohio-state.edu (Avner Friedman)

on differential equations that describe the interactions of stimuli for NF-κB activation and mitogen concentrations and allows one to make predictions about how mouse 3T3-L1 preadipocytes choose between proliferation, differentiation or quiescence. Those predictions are supported by experiments on mouse 3T3-L1 cells.

Key words: fat cell, adipogenesis, quiescence, proliferation, differentiation, PPARγ, NF-κB, Cyclin D1

Introduction

Historically, it was thought that adipose tissue served merely as a energy storage depot by sequestering esterified fatty acids in large lipid droplets (1, 2). More recently, many studies have demonstrated that white fat is a major source of adipocyte-specific adipokines (leptin, adiponectin, resistin) that orchestrate a complex communication system leading to energy homeostasis during health and disease states such as type 2 diabetes mellitus and metabolic syndrome (3, 4). In addition, pro-inflammatory cytokines (interleukin-6, IL-6; tumor necrosis factor-α, TNF-α) secreted by adipocytes and macrophages that invade adipose tissues are profoundly up-regulated in disease states such as arteriosclerosis, type 2 diabetes, obesity and the metabolic syndrome (5). Thus, it is now recognized that white fat is a highly complex tissue comprised of many cell types and pleiotropic metabolic functions. Moreover, the recruitment and differentiation of preadipocytes into fully functional adipocytes is a remarkably coordinated process involving several transcription factors and their target genes (6).

Specifically, in vitro studies have shown that proliferating preadipocytes undergo a one or two final rounds of clonal expansion prior to their initiation of the differentiation program led by a complex network of C/EBP-α and-β and the master adipogenic regulator peroxisome proliferator-activated receptor-γ (PPAR-γ) (7–9). In recent years, there has been a recognition that local inflammatory events within adipose tissue may have profound consequences in obesity, insulin resistance and type 2 diabetes (10). In addition, the central transcription factor in inflammatory cells, nuclear factor-κB (NFκB) is up-regulated in metabolic dysfunction such as type 2 diabetes and insulin resistance, and, in fact, may be a valuable target of therapeutic intervention (11). In many cell types NF-κB is an important regulator of cell proliferation and survival (12). As such we postulated that during the

final stages of preadipocyte cell growth preceding early differentiation events, NF-κB and PPAR-γ interact to govern the state of cell quiescence, proliferation and initiation of differentiation. Importantly, we have approached this problem from a theoretical perspective and have constructed a simple mathematical model to predict how environmental and/or intrinsic molecular mechanisms might regulate these processes. We also conducted experiments with results that indirectly support our model.

The differentiation of preadipocyte is regulated by a complex network of transcription factors and other proteins. The master transcription factors in adipogenesis are PPARγ and C/EBPα (6, 13, 14). Agonistic ligands for PPARγ are also shown to inhibit proliferation of T helper cell clones and B cells (15–17). It is known that there is a mutual inhibition between NF-κB and PPARγ (18–20). PPARγ, for example, inhibits cytokine-induced cytotoxicity via NF-κB (21). NF-κB in turn, through induction of TNF-α, is able to antagonize the synthesis of PPARγ, block adipocyte differentiation, and contribute to insulin resistance (22).

The role of NF-κB in these processes is actually quite complex. It controls indirect auto-inhibition and auto-activation pathways, and thus has a dual role. Through induction of COX2, NF-κB positively effects production of the prostaglandins (23–25). The prostaglandin 15d-PGJ_2 is considered to be the endogenous ligand and activator of PPARγ (26). As a result, NF-κB plays a role, although indirectly, in the activation of PPARγ. 15d-PGJ_2 and IκB, a protein which is induced by NF-κB, are both known inhibitors of NF-κB (27–29). Since, as mentioned above, NF-κB induces the potent activator, TNF-α, this process can be considered as auto activation (30).

NF-κB has positive influence on the induction of Cyclin D1 through TNF-α (31, 32). Similarly, Cyclin D1 has a positive influence on the induction of PPARγ through activation of E2F1, but it also acts as a transrepressor by recruiting HDACs to the PPAR response element (6, 33).

The model is formulated as a system of nonlinear ordinary differential equations, where most of the parameters are experimentally unknown at this time. A critical assumption of our model is that each state of the cell (quiescence, proliferation, early differentiation events) is represented by the steady-state solution of the equations contained within the model. Because of the complexity of the molecular phenomena, our initial mathematical model considers only three principal components: NF-κB, PPAR-γ and cyclin D (23, 34). Our equations predict that the most important parameter in the fate decision making by the preadipocyte is the rate of autoinhibition of NF-

kB through the induction of IκB (NF-κB autoinhibitor). The parameters of secondary importance are the induction or degradation of PPAR-γ and cyclin D1. In the interest of simplicity, the induction rate of cyclin D1, k_8, was selected as the second parameter for the analysis. Bifurcation diagrams based on the model equations demonstrate how the relative strengths of these two parameters determine the fate of the precursor cell. This simplified, first principles model may be useful in predicting how cells orchestrate the complex decision making of remaining quiescent, undergoing proliferation or differentiate into functional tissue cells.

1. The Model

We denote by x_1, x_2, and x_3, the concentrations of NF-κB, Cyclin D1, and PPARγ, respectively. The diagram in Fig. 1 illustrates the relations described in the introduction and summarized in Table 1.

A single line in the figure represents activation or inhibition; a double line, induction or production; an arrow head stands for positive interaction, and a blunt head stands for negative interaction. Since the model does not distinguish between active and inactive forms of the proteins, single and double lines are considered to be the same in the mathematical formulation of the model. The relations indicated in Fig. 1 are mainly indirect mechanisms of molecular interactions.

The diagram in Fig.1 is expressed by the following system of differential equations:

$$\frac{dx_1}{dt} = k_1 \frac{x_1^2}{j_1^2 + x_1^2} \frac{k_2}{k_2 + x_1} \frac{k_3}{k_3 + x_3} - k_4 x_1 + k_5 \tag{1}$$

$$\frac{dx_2}{dt} = k_6 \frac{x_1}{j_2 + x_1} - k_7 x_2 + k_8 \tag{2}$$

$$\frac{dx_3}{dt} = k_9 \frac{x_1}{j_3 + x_1} \frac{k_{10}}{k_{10} + x_1} + k_{11} \frac{x_2}{j_4 + x_2} \frac{k_{12}}{k_{12} + x_2} - k_{13} x_3 + k_{14} \tag{3}$$

For NF-κB dynamics in Eq. 1, two step Hill kinetics is used for auto-activation in the first factor of the first term; the second and third factors represent auto-inhibition and inhibition by PPARγ, respectively. Eq. 1 also includes a degradation term, $-k_4 x_1$, and an induction term, k_5.

For Cyclin D1 dynamics in Eq. 2, the first term represents induction by NF-κB, the second term, $-k_7 x_2$, accounts for degradation, and the last term, k_8, is induction by factors other than NF-κB.

For PPARγ dynamics in Eq. 3, the first term accounts for activation (through COX2 and 15d-PGJ_2) and inactivation by NF-κB. Similarly the second term represents activation and inactivation of PPARγ by Cyclin D1. As before, a degradation, $-k_{13}x_3$, and an induction term, k_{14}, are assumed.

It is known that the inactivation of NF-κB is mainly due to the IκB concentration (28, 29), and induction of Cyclin D1 is due to mitogenic stimulation (6). Based on these facts, it is reasonable to assume that the auto-inactivation parameter k_2 for NF-κB is a decreasing function of IκB concentration, and the parameter of Cyclin D1 induction, k_8, is an increasing function of mitogen concentration in the cell.

Results

It is assumed that a decision about the state of the cell, i.e., whether to differentiate along the adipocyte lineage, proliferate, or remain in a quiescent state, is expressed by the equilibrium state of the system of Eqs. 1-3, that is, by

$$\frac{dx_1}{dt} = \frac{dx_2}{dt} = \frac{dx_3}{dt} = 0. \tag{4}$$

Based on this assumption, a jump from one branch to another at a bifurcation point along the curve of equilibrium points is interpreted as a change in the state of the cell.

Eqs. 4 are numerically solved for the equilibrium points (x_1, x_2, x_3) for varying values of the parameters k_2 and k_8, using the software XPPAUT. The choice of k_2 as a bifurcation parameter is due to an important model prediction that, bifurcation phenomena (the change in the state of the cell) occurs for only for a certain range of k_2, as explained below. The other bifurcation parameter k_8 is arbitrarily chosen from the set of degradation and induction parameters, namely, $\{k_4, k_5, k_7, k_8, k_{13}, k_{14}\}$. For the purpose of illustration, all parameters are fixed as in Table 2, except k_2 and k_8. It should be noted however that although the parameter set was arbitrarily chosen, the subsequent analysis does not appear to depend on the choice of the particular parameters. The dependence of the state of the cell on the parameters k_2 and k_8 is analyzed in what follows.

In the figures below, the states of quiescence, differentiation, and proliferation are represented by Q, D, and P in the given order. The stable and unstable states are indicated by superscripts s and u, respectively. The con-

tinuation of stable equilibrium points are plotted with solid lines and that of the unstable equilibrium points with dashed lines.

Fig. 2(a) profiles the x_1, x_2, and x_3 components of the equilibrium points as functions of the parameter k_2 when $k_8 = 1$, and Fig. 2(b) profiles these components as functions of the parameter k_8 for $k_2 = 6$.

In Fig. 2(a), the stable upper and lower branches are connected by the unstable middle branches at the bifurcation points V_1 and V_2, represented by red, solid circles. The fact that PPARγ is the master regulator of adipocyte differentiation is used for the determination of the state of the cells: on the (x_3, k_2) curve, (and consequently on the corresponding branches of the other curves of Fig. 2(a)) the stable upper branch is identified by the differentiation state, D^s, because of the high equilibrium concentration level of PPARγ, and the stable lower branch is identified by either proliferation, P, or quiescence, Q, states, (Q, P). Apparently k_2 does not distinguish between P and Q states. Additional information through analysis of the system with respect to the parameter k_8 will be employed on, in Fig. 4, in order to distinguish between the states P and Q.

As k_2 increases from 0 to $k_{2,2} = 6.947$, where the bifurcation point V_2 resides, the cell assumes D^s state. Upon surpassing $k_{2,2}$, the cell's state changes to $(Q, P)^s$. The cell remains in this state as long as k_2 remains larger than $k_{2,1} = 5.981$ where the bifurcation point V_1 resides. If k_2 is further decreased, the cell goes back to the D^s state. This phenomena of coexistence of the states D^s and $(Q, P)^s$ in an overlapping interval, in this case $k_{2,1} < k_2 < k_{2,2}$, is called *hysteresis*.

In Fig. 2(b), where the profiles of the x_i are shown as functions of k_8 when $k_2 = 6$, there are four bifurcation points, denoted by Y_1, Y_2, Y_3, and Y_4 and represented by blue, solid diamonds on the graphs. In order to use these profiles to determine the cell state, the following facts were used: (i) NF-κB concentration decreases (most likely its active form, see Discussion) during differentiation, (ii) increased Cyclin D1 level is associated with proliferation, and (iii) as mentioned previously, PPARγ is the master regulator of adipogenesis. The low equilibrium concentration of PPARγ and Cyclin D1 for small values of k_8 suggest the identification of the first, stable branches ending in Y_2 by quiescence, Q^s. The high concentration level of PPARγ on (x_3, k_8), and low concentration of NF-κB on (x_1, k_8) graph suggest identification of middle, stable branches (Y_1Y_4) by differentiation, D^s. High equilibrium concentration of Cyclin D1 and low concentration of PPARγ imply the identification of the third, stable branches starting at the bifurcation point Y_4 by

proliferation, P^s.

Fig. 3 depicts (x_1, k_8) curves for three different values of k_2. The behavior of the graphs indicates that the bifurcation points Y_1 and Y_3 are approaching each other as k_2 increases, and eventually coalesce at the point Z_1 for $k_2 = 7.6017$ and $k_8 = 3.6435$ on the parameter space (k_8, k_2) (see Figs. 3(a)-3(c)). This point Z_1 will be called as *point of uncertainty*. For increasing values of k_2, points of uncertainty, Z, define *the curve of uncertainty*, which will be denoted by ϕ on Fig. 4 and Fig. 3(d).

The graphs of Fig. 2 and Fig. 3 are prototypical examples for specific values of k_2 and k_8. Fig 4, however, summarizes the correspondence between the curves of bifurcation points and different states of the cell together with their stability on the (k_8, k_2) parameter space. There are several observations to be made on Fig. 4.

First, the model predicts that, bifurcation phenomena occur only when k_2 is within a certain range, more specifically,

$$k_{2,min} = 3.7787 < k_2 < 12.5837 = k_{2,max}.$$

The parameter k_2 also determines the number of bifurcation points. There are four bifurcation points along the parameter k_8 when $4.3768 < k_2 < 7.6017$. For $7.6017 < k_2 < 12.5837$ two of these bifurcation points, Y_2 and Y_4, coalesce into one equilibrium point, Z (see Fig. 3). So, in this interval, and also when $3.783 < k_2 < 4.3768$, there are only two bifurcation points along k_8. The number of bifurcation points along the parameter k_2 is always two within the range $k_{8,min} = 0.1614 < k_8 < 28.48 = k_{8,max}$. There are no bifurcation points outside of the ranges specified above.

The region enclosed by the dashed, closed bifurcation curves ψ in Fig. 4 is the region of three state coexistence. This region will be referred to as *region of uncertainty*, and will be denoted by U. The curve of uncertainty, ϕ, separates this region into two parts; in the left half subregion Q^s, D^s, Q^u or D^u coexist, while in the right subregion the existing states are D^s, P^s, D^u or P^u. The importance of the curve of uncertainty is in that for $7.6017 < k_2 < 12.5837$, and $(k_2, k_8) \in U$, a cell may immediately transit from Q^s to P^s state by crossing ϕ with increasing values of k_8, without a differentiation stage. The cell may assume D^s state in the region of uncertainity.

The region left and right to the uncertainty region are predominantly single state regimes of stable quiescence, Q^s, and proliferation states, P^s, respectively. These regions may be called *regions of stable quiescence* and

stable proliferation, respectively. In a similar manner, the single state *region of stable differentiation* lies below the uncertainty region, and is characterized by relatively small values of both k_2 and k_8 (see Fig. 4).

For the specific parameters chosen in Table 2, the quantitative characterization of U (enclosed by ψ), ϕ, and of Z_1 are given as follows:

Let n_1 and d_1 are given by:

$$n_1 = \left(10\,{k_8}^2 + (10 - 40\sqrt{5})k_8 + 980\sqrt{5} - 2077\right)\left(65{k_8}^2 + (128 - 260\sqrt{5})k_8 - 256\sqrt{5} + 1364\right)$$
$$(k_8 - 2\sqrt{5})(2k_8 + 1 - 4\sqrt{5}),$$

$$d_1 = 2\,(1 - 2\sqrt{5} + k_8)(1300{k_8}^5 + (4510 - 13000\sqrt{5}){k_8}^4 + (-31040 + 93920\sqrt{5}){k_8}^3$$
$$+ (-4087317 + 1547240\sqrt{5}){k_8}^2 + (-21864672 + 10248468\sqrt{5})k_8 - 41472068 + 18250144\sqrt{5}).$$

Then, the curve of uncertainty, ϕ, as a function of k_8, is:

$$\phi(k_8) = \frac{n_1}{d_1}, \quad 3.6469 < k_8 < 3.7779. \tag{5}$$

The points, Z, on ϕ are not bifurcation points. The end points of ϕ are $Z_1 = (7.6016, 3.6469)$, and $Z_2 = (12.5836, 3.7779)$. It should be noted that on ϕ, a cell may assume one of the three stable states while the number of possible states along ψ, including Z_1 and Z_2, is only two.

Let K_2 be a function of k_8, and depend on x_1 as a parameter, defined by:

$$K_2(k_8, x_1) = \frac{n_2}{d_2},$$

where

$$n_2 = -x_1(2\,x_1 - 1)({x_1}^2 + 16)\left((432\,{x_1}^4 + 944\,{x_1}^3 + 728\,{x_1}^2 + 236\,x_1 + 27){k_8}^2\right.$$
$$+ (8752\,{x_1}^4 + 17952\,{x_1}^3 + 13280\,{x_1}^2 + 4232\,x_1 + 493)k_8$$
$$\left.+16960\,{x_1}^4 + 31944\,{x_1}^3 + 20944\,{x_1}^2 + 5706\,x_1 + 540\right),$$

$$d_2 = (-11264\,{x_1}^5 + 3840\,{x_1}^4 + 1610\,{x_1}^3 - 11344\,{x_1}^6 - 2912\,x_1 - 4923\,{x_1}^2 - 432 + 864\,{x_1}^7){k_8}^2$$
$$+ (19872\,{x_1}^5 + 237616\,x1^4 - 7888 - 51936\,x_1 - 84749\,{x_1}^2 + 73682\,{x_1}^3 + 17504\,{x_1}^7 - 113648\,{x_1}^6)k_8$$
$$+ 12078\,{x_1}^3 + 267716\,{x_1}^4 - 144936\,{x_1}^5 - 337072\,{x_1}^6 + 33920\,{x_1}^7 - 74016\,x_1 - 169052\,{x_1}^2 - 8640.$$

For $\Lambda_{x,y}$ being the region enclosed by two curves $K_2(k_8, x)$ and $K_2(k_8, y)$ when $1.1350 < x, y < 2.3599$, $x \neq y$, the region of uncertainty U can then be described as:

$$U = \bigcup_{\substack{x,y \\ x \neq y}} \Lambda_{x,y}, \quad 1.1350 < x, y < 2.3599. \tag{6}$$

In other words, there are two intersection points of the graphs of $K_2(k_8, x)$ and $K_2(k_8, y)$ with the conditions on x and y as given in Eq. 6, and these intersection points determine the curve ψ.

Although the above formulas for U and ϕ were obtained for the specific parameters given in Table 2, similar formulas can be determined for any other set of parameters.

Discussion

A comprehensive understanding of adipose tissue development and its role in energy metabolism and endocrine signaling is of paramount importance given that molecular derangements during adipogenesis can have profound pathophysiological consequences as seen in obesity, insulin resistance and type 2 diabetes (35, 36). The present work addresses in a predictive fashion the question of preadipocyte cell fate determination, and how fat cell precursors utilize intrinsic and extrinsic information to "decide" whether to proliferate, differentiate into mature adipocytes, or remain in a quiescent state. For simplicity, in this initial modeling endeavor, we did not consider the fourth decision, that is, apoptosis. Further refinements of the model will have to take this latter cellular state into consideration. The paper develops, for the first time, a mathematical model which predicts how a preadipocyte determines whether to proliferate, differentiate, or remain in quiescent state. Only three main components were considered in this initial modeling effort: NF-κB, cyclin D1, and PPAR-γ. To our knowledge, this is the first paper to directly address the potential role of NF-κB in the proliferative and differentiation phases of preadipocytes. However, the role of NF-κB in cell proliferation and differentiation was considered in several studies in other cell systems, including vascular smooth muscle cells, breast cancer cells, and B lymphocytes (17, 37, 38).

As summarized in Fig. 4, the model provides a quantitative measure in predicting the adipocyte precursor fate and a tool in predicting the behavior of preadipocytes during the early stages of adipogenesis. The region of uncertainty, U, enclosed by ψ, is the position at which the preadipocyte can assume two different stable states: to the left of the curve of uncertainty, ϕ, stable differentiation and quiescence states, and to the right of ϕ stable differentiation and proliferation states. The region left of, right of, and below the region of uncertainty, U, are single stable quiescence, proliferation, and differentiation states, respectively. Although the parameters are currently

largely unknown experimentally, the results obtained in Fig. 4 suggest novel approaches for new experiments to investigate cell fate determination. For example, based on the qualitative nature of the region of uncertainty U shown in Fig. 4, one could modulate the parameters k_2 and k_8 in order to arrest the cell in a quiescent state as a potential means of controlling obesity and its consequences (type 2 diabetes, insulin resistance, metabolic syndrome).

The parameter, k_2, which represents IκB concentration, or NF-κB inactivation (autoinhibition), and k_8, which represents the strength of mitogenic stimulus are important elements of the model. Future experiments will test whether this prediction is empirically the case. That is, to validate the importance of k_2 (i.e., the extent of NF-κB activity), it will be critical to know if the inhibition rate of NF-κB is vital for cell proliferation, differentiation or quiescence during the early stages of adipogenesis. In fact, there is some evidence in the literature that supports a role for NF-κB in cell proliferation. Vascular smooth muscle cell proliferation, for example, a crucial event in the formation of atherosclerotic plaques, is regulated by NF-κB and its inhibitor IκB-α (38). Hsieh et al. (37) demonstrated that NF-κB was critically involved in controlling the growth of several breast cancer cell lines in response to Chinese herbal formulations. Finally, using IκB kinase $\beta^{-/-}$ mice, Ren et al. (39) reported that B cell proliferation and subsequent antibody production following exposure to lipopolysaccharide was severely diminished, implicating NF-κB activation in lymphocyte cell cycle control.

Our experimental data (see the Experimental Data section) demonstrated that, in preadipocytes stimulated with TNF-α, there was a time-dependent diminution in IκB-α and a concomitant increase in p65 activation, which is presumptive evidence in support of our simplified model. Interestingly, we detected no substantial difference in undifferentiated 3T3-L1 cells compared to cells undergoing early stages of differentiation (i.e., within 2 days following addition of the IDX cocktail), that is, following the up-regulation of PPAR-γ. It was recently reported that adipogenesis is associated with changes in amount and subunit composition of the NF-κB complexes. NF-κB subunits p65/RelA, RelB, and IκB-α are up-regulated during fat cell differentiation (40). We did not detect such a dramatic increase in the absolute amount of p65, Rel B or IκB-α (data not shown). Rather, cells retained their ability to respond to TNF-α by enhanced IκB-α phosphorylation and degradation without a major impact on the steady-state level of IκB-α. Since localized inflammation within adipose tissue can be elicited by infiltrating macrophages in response to cytokines (TNF-α and IL-6), it is likely that the case that the

activation status of NF-κB is crucial the recruitment and differentiation of preadipocytes within white fat in pathological settings (e.g., obesity-related insulin resistance) (41). Since our initial model does not specifically delineate between active and inactive forms of NF-κB, this result does not contradict the prediction of low levels of NF-κB concentration in (x_1, k_8) graph of Fig. 2. There is some experimental support for the possibility that NF-κB function decreases as differentiation proceeds (42). Thus, the steady-state concentration of NF-κB is consistent with the model predictions.

Fig. 4 displays the steady state of the model system Eq. 3 for preadipocyte fate determination in terms of the parameters k_2 and k_8. A similar figure can be obtained in terms of k_2 and k_{14}. Here k_{14} is a parameter representing induction of PPARγ or, equivalently, the effect of insulin on PPARγ induction (43). A recent paper by Guo et al. (44) provides evidence that the early events in preadipocyte commitment toward the adipogenesis pathway can be segregated into two distinct stages, i.e., licensing of adipocyte formation and execution of the terminal differentiation program. The licensing stage can be identified with the quiescence stage in our paper. Their results suggest that differentiation licensing and differentiation execution can be uncoupled and separately linked to cell proliferation. As a matter of fact, Fig. 4 with (k_2, k_{14}) instead of (k_2, k_8), provides a quantitative measure for mutual relations among Q^s, P^s and D^s based on the NFκB inhibition (k_2) and PPARγ induction or insulin administration (k_{14}) coefficients. Their result that, when the licensed 3T3-L1 cells were treated only with insulin, the adipogenesis commitment could be maintained from one cell generation to the next, whereby the licensed program could be activated in a cell-cycle-independent manner once these cells were subjected to adipogenesis-inducing conditions, can be translated into the terminology of our results by stating that cells can switch from Q^s to a stable differentiation stage D^s across the curve of uncertainty, ϕ, based on the strength of insulin treatment k_{14} (when k_{14} is used instead of k_8). Moreover, cell contact inhibition and subsequent reentry into mitotic clonal expansion are pivotal for this biphasic process. Now, our model that includes a description of the potential role of NFκB in these events can be tested further.

As mentioned earlier, we selected only three principal molecular factors for the sake of simplicity, but we are fully cognizant that as the model evolves an increasing degree of complexity will be introduced. For example, we have only considered the canonical NF-κB pathway (45) in this model. A greater appreciation of the subunit contribution of NF-κB (i.e., p65, RelB,

c-Rel, and p50) (46–48), both isoforms of PPAR-γ (PPAR-γ1 and -γ2) (49), and eventually different external agents (cytokines (NF-κB activators) and mitogens (insulin, insulin-like growth factor-I) (50) need to be considered separately for their importance and function in adipocyte biology.

Finally, extensive experimental validation of the simplified and future generations of the model must be undertaken to assess the utility of this mathematical approach in predicting preadipocyte fate decision making. It will also be interesting to employ the model in other cell types, such as various stem cell populations.

Materials and Methods

Cell culture

Mouse 3T3-L1 fibroblasts were obtained from the American Type Culture Collection and cultured in Dulbecco's minimal essential medium (DMEM) supplemented with 2 mM L-glutamine, 10% bovine calf serum (FBS) and antibiotics as previously described (23, 51). After 2 days in vitro, cells were rinsed with serum-free DMEM and then transferred to differentiation medium (insulin, dexamethasone and isobutylmethylxanthine, IDX) as previously described (23).

Immunoblotting

Cellular proteins were extracted using RIPA lysis buffer supplemented with a protease and phosphatase inhibitor cocktail (Sigma) and quantified by the Biorad assay using bovine serum albumin (BSA, Sigma) as standard. Approximately 30 μg/lane were loaded onto 10% sodium dodecyl sulfate-polyacrylamide gels (SDS-PAGE) followed by transfer to nitrocellulose membranes (Hybond, Amersham). After thorough blocking of non-specific binding with Tris-buffered saline/Tween-20 (TBST) containing 5% nonfat dry milk for 1 hour, membranes were incubated overnight at 4C, followed by washing with TBST/5% nonfat dry milk and incubation with secondary antibodies diluted 1:2000 with TBST/5% nonfat dry milk for 1 hour, and visualized using a VersaDoc Imaging System (Biorad).

Experimental Data

To investigate the elements of the mathematical model presented here, we conducted immunoblotting studies to determine the relative time-course and signal strength of IκB-α phosphorylation and degradation as a surrogate

for NF-κB activation. Mouse 3T3-L1 cells were incubated in the presence or absence of IDX differentiation cocktail 2 days after plating, and after an additional 2 days they were exposed to 5 or 30 min with TNF-α (50 ng/ml) or lipopolysaccharide (LPS, 10 μg/ml). Immunoblots prepared from total cell extracts were fractionated by SDS-PAGE, transferred to nitrocellulose membranes and probed with antibodies directed against IκB-α, p65, IκB kinase (IKK), or PPAR-γ. As shown in Fig. 5, treatment with TNF-α led to a rapid (within 5 min) increase in IκB-α phosphorylation and a concomitant diminution in total IκB-α protein. In addition, TNF-α stimulation prompted the appearance of phospho-p65 subunit, a marker of NF-κB activation. When cells were treated with TNF-α there was also a rapid increase in phosphorylation of the a and b subunits of IKK, the heterodimeric kinase responsible for IκB-α phosphorylation and subsequent degradation leading to NF-κB activation. LPS, although clearly a stimulus of the NF-κB pathway, was much less effective relative to TNF-α (Fig. 5).

References

[1] G. Ailhaud, P. Grimaldi, R. Negrel, Cellular and molecular aspects of adipose tissue development, Annual Review of Nutrition 12 (1992) 207–33.

[2] D. A. Bernlohr, A. E. Jenkins, B. A. A., Adipose tissue and lipid metabolism, Biochemistry of lipids, lipoproteins and membranes 36 (2004) 263–89, bernlohr, D. A., A. E. Jenkins, and A. A. Bennaars. "Adipose Tissue and Lipid Metabolism." Biochemistry of lipids, lipoproteins and membranes. Ed. D. E. Vance and C. Vancheri. 4th ed. New comprehensive biochemistry vol. 36. Ed. G. Bernardi. Amsterdam: Elsevier, 2004.

[3] J. L. Miner, The adipocyte as an endocrine cell, Journal of Animal Science 82 (2004) 935–41.

[4] P. E. Scherer, Adipose tissue: from lipid storage compartment to endocrine organ, Diabetes 55 (2006) 1537–45.

[5] S. E. Shoelson, J. Lee, A. B. Goldfine, Inflammation and insulin resistance, Journal of Clinical Investigation 116 (2006) 1793–801.

[6] S. R. Farmer, Transcriptional control of adipocyte formation, Cell Metabolism 4 (4) (2006) 263–273.

[7] Q.-Q. Tang, T. C. Otto, M. D. Lane, Ccaat/enhancer-binding protein b is required for mitotic clonal expansion during adipogenesis, Proceedings of the National Academy of Sciences 100.3 (2003) 850–55.

[8] Q.-Q. Tang, T. C. Otto, M. D. Lane, Mitotic clonal expansion: A synchronous process required for adipogenesis, Proceedings of the National Academy of Sciences 100.1 (2003) 44–49.

[9] S. M. Rangwala, M. A. Lazar, Transcriptional control of adipogenesis, Annual Review of Nutrition 20 (2000) 535–59.

[10] K. E. Wellen, G. S. Hotamisligil, Obesity-induced inflammatory changes in adipose tissue, Journal of Clinical Investigation 112.12 (2003) 1785–88.

[11] M. Yuan et. al., Reversal of obesity- and diet-induced insulin resistance with salicylates or targeted disruption of ikkb, Science 293 (2001) 1673–77.

[12] M. Karin, A. Lin, Nf-kb at the crossroads of life and death, Nature Immunology 3.3 (2002) 221–27.

[13] E. D. Rosen, C.-H. Hsu, X. Wang, S. Sakai, M. W. Freeman, F. J. Gonzalez, B. M. Spiegelman, C/EBPalpha induces adipogenesis through PPARgamma : a unified pathway, Genes Dev. 16 (1) (2002) 22–26.

[14] E. D. Rosen, B. M. Spiegelman, Molecular regulation of adipogenesis, Annual Review of Cell and Developmental Biology 16 (1) (2000) 145–171.

[15] R. B. Clark, D. Bishop-Bailey, T. Estrada-Hernandez, T. Hla, L. Puddington, S. J. Padula, The nuclear receptor ppargamma and immunoregulation: Ppargamma mediates inhibition of helper t cell responses, J Immunol 164 (3) (2000) 1364–1371.

[16] X. Y. Yang, L. H. Wang, T. Chen, D. R. Hodge, J. H. Resau, L. DaSilva, W. L. Farrar, Activation of human t lymphocytes is inhibited by peroxisome proliferator-activated receptor gamma (ppargamma) agonists.

ppargamma co-association with transcription factor nfat, J. Biol. Chem. 275 (7) (2000) 4541–4544.

[17] K. Setoguchi, Y. Misaki, Y. Terauchi, T. Yamauchi, K. Kawahata, T. Kadowaki, K. Yamamoto, Peroxisome proliferator-activated receptor-γ haploinsufficiency enhances b cell proliferative responses and exacerbates experimentally induced arthritis, J. Clin. Invest. 108(11) (2001) 1667–1675.

[18] A. A. Beg, ComPPARtmentalizing NF-[kappa]B in the gut, Nat Immunol 5 (1) (2004) 14–16.

[19] S. W. Chung, B. Y. Kang, S. H. Kim, Y. K. Pak, D. Cho, G. Trinchieri, T. S. Kim, Oxidized low density lipoprotein inhibits interleukin-12 production in lipopolysaccharide-activated mouse macrophages via direct interactions between peroxisome proliferator-activated receptor-gamma and nuclear factor-kappa b, J. Biol. Chem. 275 (42) (2000) 32681–32687.

[20] M. Ricote, A. C. Li, T. M. Willson, C. J. Kelly, C. K. Glass, The peroxisome proliferator-activated receptor-[gamma] is a negative regulator of macrophage activation, Nature 391 (6662) (1998) 79–82.

[21] E.-K. Kim, K.-B. Kwon, B.-S. Koo, M.-J. Han, M.-Y. Song, E.-K. Song, M.-K. Han, J.-W. Park, D.-G. Ryu, B.-H. Park, Activation of peroxisome proliferator-activated receptor-[gamma] protects pancreatic [beta]-cells from cytokine-induced cytotoxicity via nf[kappa]b pathway, The International Journal of Biochemistry & Cell Biology 39 (6) (2007) 1260–1275.

[22] C. Jiang, A. T. Ting, B. Seed, Ppar-[gamma] agonists inhibit production of monocyte inflammatory cytokines, Nature 391 (6662) (1998) 82–86.

[23] Y. Xie, X. Kang, W. E. Ackerman, M. A. Belury, C. Koster, B. H. Rovin, M. B. Landon, D. A. Kniss, Differentiation-dependent regulation of the cyclooxygenase cascade during adipogenesis suggests a complex role for prostaglandins, Diabetes, Obesity and Metabolism 8 (1) (2006) 83–93.

[24] D. A. Kniss, B. Rovin, R. H. Fertel, P. D. Zimmerman, Blockade nf-[kappa]b activation prohibits tnf-[alpha]-induced cyclooxygenase-2 gene expression in ed27trophoblast-like cells, Placenta 22 (1) (2001) 80–89.

[25] D. Kniss, Cyclooxygenases in reproductive medicine and biology, Journal of the Society for Gynecologic Investigation Pages 6(6) (1999) 285 – 292.

[26] B. M. Forman, P. Tontonoz, J. Chen, R. P. Brun, B. M. Spiegelman, R. M. Evans, 15-deoxy-[delta]12,14-prostaglandin j2 is a ligand for the adipocyte determination factor ppar[gamma], Cell 83 (5) (1995) 803–812.

[27] W. E. I. Ackerman, X. L. Zhang, B. H. Rovin, D. A. Kniss, Modulation of cytokine-induced cyclooxygenase 2 expression by pparg ligands through nfkappab signal disruption in human wish and amnion cells, Biol Reprod 73 (3) (2005) 527–535.

[28] A. Y. Ting, D. Endy, Signal transduction: Decoding nf-kb signaling, Science 298 (5596) (2002) 1189–1190.

[29] A. Hoffmann, A. Levchenko, M. L. Scott, D. Baltimore, The ikappa b-nf-kappa b signaling module: Temporal control and selective gene activation, Science 298 (5596) (2002) 1241–1245.

[30] S. Beinke, S. C. Ley, Functions of nf-kappab1 and nf-kappab2 in immune cell biology., Biochem. J. 382 (2) (2004) 393–409.

[31] W. P. Cawthorn, F. Heyd, K. Hegyi, J. K. Sethi, Tumour necrosis factor-[alpha] inhibits adipogenesis via a [beta]-catenin//tcf4(tcf7l2)-dependent pathway, Cell Death Differ 14 (7) (2007) 1361–1373.

[32] A. Kikuchi, Regulation of [beta]-catenin signaling in the wnt pathway, Biochemical and Biophysical Research Communications 268 (2) (2000) 243–248.

[33] M. Fu, M. Rao, T. Bouras, C. Wang, K. Wu, X. Zhang, Z. Li, T.-P. Yao, R. G. Pestell, Cyclin d1 inhibits peroxisome proliferator-activated receptor gamma-mediated adipogenesis through histone deacetylase recruitment, J. Biol. Chem. 280 (17) (2005) 16934–16941.

[34] A. Abella et al, Cdk4 promotes adipogenesis through pparg activation, Cell Metabolism 2 (2005) 239–49.

[35] H. Waki, P. Tontonoz, Endocrine functions of adipose tissue, Annual Review of Pathology and Mechanisms of Disease 2 (2007) 31–56.

[36] M. I. Lefterova, M. A. Lazar, New developments in adipogenesis, Trends in Endocrinology and Metabolism 20.3 (2009) 107–14.

[37] T.-c. Hsieh, E. K. Wijeratne, J.-y. Liang, A. L. Gunatilaka, J. M. Wu, Differential control of growth, cell cycle progression, and expression of nf-[kappa]b in human breast cancer cells mcf-7, mcf-10a, and mda-mb-231 by ponicidin and oridonin, diterpenoids from the chinese herb rabdosia rubescens, Biochemical and Biophysical Research Communications 337 (1) (2005) 224–231.

[38] S. Hoshi, M. Goto, N. Koyama, K.-i. Nomoto, H. Tanaka, Regulation of vascular smooth muscle cell proliferation by nuclear factor-kappa b and its inhibitor, i-kappa b, J. Biol. Chem. 275 (2) (2000) 883–889.

[39] H. Ren, A. Schmalstieg, D. Yuan, R. B. Gaynor, I-kappab kinase beta is critical for b cell proliferation and antibody response, J Immunol 168 (2) (2002) 577–587.

[40] A. H. Berg, Y. Lin, M. P. Lisanti, P. E. Scherer, Adipocyte differentiation induces dynamic changes in NF-kappaB expression and activity, Am J Physiol Endocrinol Metab 287 (6) (2004) E1178–1188.

[41] E. D. Rosen, O. A. MacDonald, Adipocyte differentiation from the inside out, Nature Reviews-Molecular Cell Biology 7 (2006) 885–96.

[42] S. Chung, K. LaPoint, K. Martinez, A. Kennedy, M. Boysen Sandberg, M. K. McIntosh, Preadipocytes mediate lipopolysaccharide-induced inflammation and insulin resistance in primary cultures of newly differentiated human adipocytes, Endocrinology 147 (11) (2006) 5340–5351.

[43] D. J. Klemm, J. W. Leitner, P. Watson, A. Nesterova, J. E.-B. Reusch, M. L. Goalstone, B. Draznin, Insulin-induced adipocyte differentiation. activation of creb rescues adipogenesis from the arrest caused by inhibition of prenylation, J. Biol. Chem. 276 (30) (2001) 28430–28435.

[44] W. Guo, K.-M. Zhang, K. Tu, Y.-X. Li, L. Zhu, H.-S. Xiao, Y. Yang, J.-R. Wu, Adipogenesis licensing and execution are disparately linked to cell proliferation, Cell Res 19 (2) (2009) 216–223.

[45] S. Ghosh, M. Karin, Missing pieces in the nf-kb puzzle, Cell 109 (2002) S81–S96.

[46] C. L. Hayes, S. Ghosh, Shared principles in nf-kb signaling, 132 132 (2008) 344–62.

[47] e. a. Lipniacki, T., Mathematical model of nf-kb regulatory module, Journal of Theoretical Biology 228 (2004) 195–215.

[48] R. Cheong, A. Levchenko, Wires in the soup: quantitative models of cell signaling, Trends in Cell Biology 2008 (2008) 112–18.

[49] P. Tontonoz, B. M. Spiegelman, Fat and beyond: The diverse biology of pparg, Annual Review of Biochemistry 77 (2008) 289–312.

[50] F. M. Gregoire, Adipocyte differentiation: From fibroblast to endocrine cell, Experimental Biology and Medicine 226.11 (2001) 997–1002.

[51] H. Green, O. Kehinde, Sublines of mouse 3t3 cells that accumulate lipid, Cell 1 (1974) 113–18.

Figure Legends

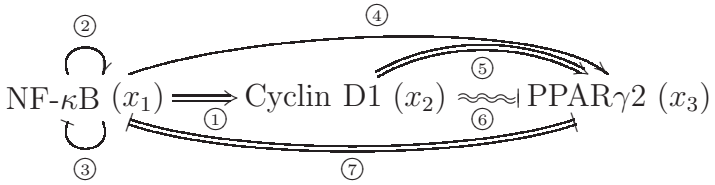

Figure 1: Biological model of indirect molecular interactions.

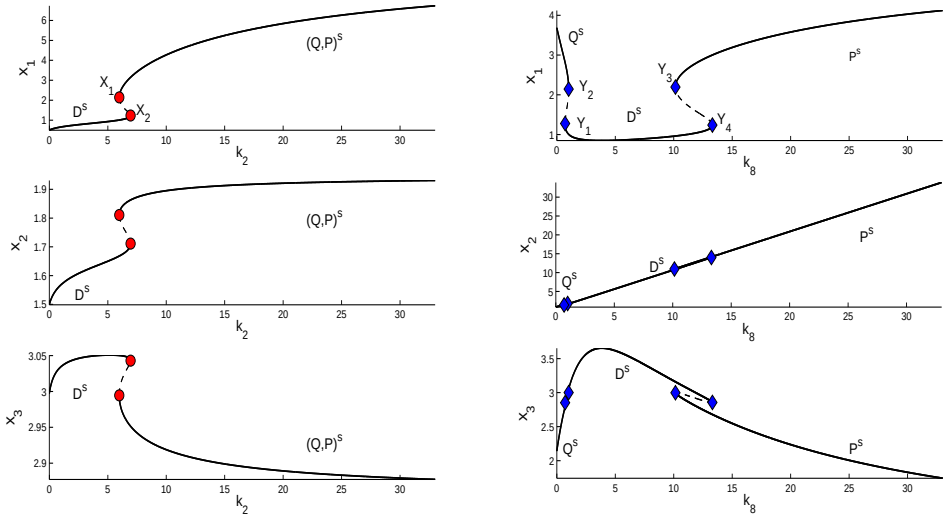

(a) x_i's vs k_2 for $k_8 = 1$ (b) x_i's vs k_8 for $k_2 = 6$

Figure 2: The components of the equilibrium points along the parameters (a) k_2 and (b) k_8

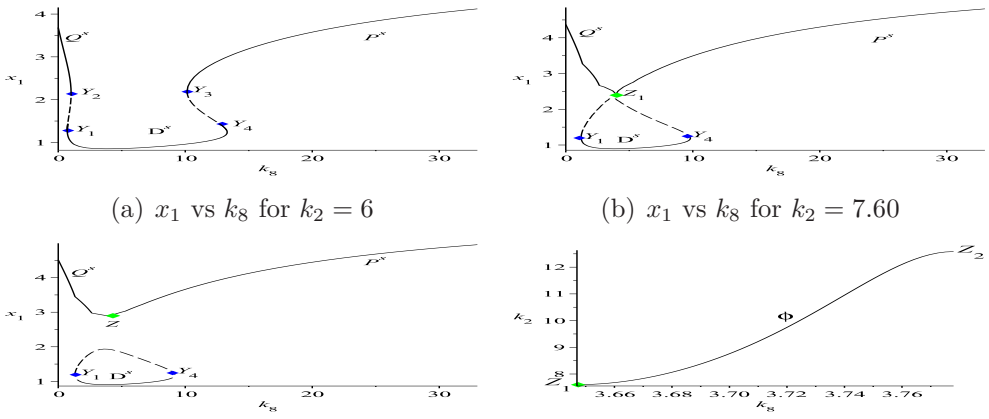

(a) x_1 vs k_8 for $k_2 = 6$

(b) x_1 vs k_8 for $k_2 = 7.60$

(c) x_1 vs k_8 for $k_2 = 8$

(d) Curve of uncertainty

Figure 3: Formation of the point (Z_1) and the curve (ϕ) of uncertainty

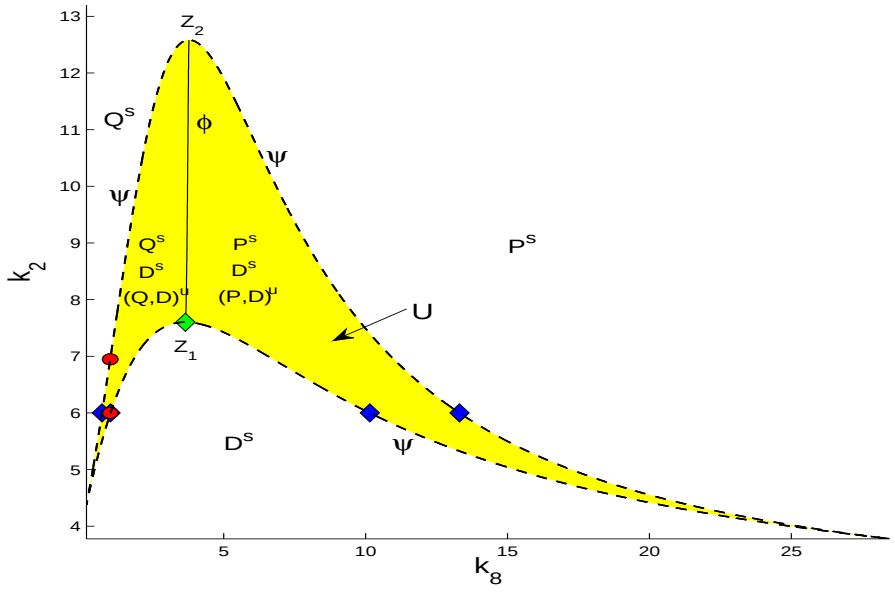

Figure 4: Region (U), curve (ϕ), and point (Z) of uncertainty

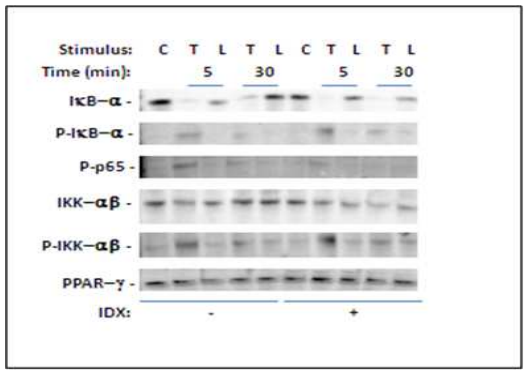

Figure 5: Mouse 3T3-L1 cells were incubated for 2 days in the presence or absence of IDX cocktail, and then challenged with TNF-α (50 ng/ml) or serum-free DMEM alone for 30 min. Cell extracts were fractionated by SDS-PAGE and immunoblots were probed with antibodies directed against phospho- or dephospho- IκB-α. The blot is representative of two similar experiments.

Tables

Table 1: References for Fig. 1

#	Relations	References
1	induction	(31), (32)
2	auto-activation	(30)
3	auto-inhibition	(27), (28), (29)
4	activation	(26), (24), (23), (25)
5	induction	(6)
6	trans-repression	(33)
7	mutual-inhibition	(21), (18), (20), (19)

Table 2: An arbitrary set of parameter values

$k_1 = 1.6$	$k_3 = 5$	$k_4 = 0.1$	$k_5 = 0.05$	$k_6 = 1$	$k_7 = 1$	$k_9 = 1$	$k_{10} = 0.5$
$k_{11} = 5$	$k_{12} = 5$	$k_{13} = 0.5$	$k_{14} = .2$	$j_1 = 4$	$j_2 = 0.5$	$j_3 = 0.5$	$j_4 = 4$